# A Cyclic Nucleotide Modulated Prokaryotic $K^+$ Channel

Crina M. Nimigean, Tania Shane, and Christopher Miller

Department of Biochemistry, Howard Hughes Medical Institute, Brandeis University, Waltham, MA 02454

ABSTRACT A search of prokaryotic genomes uncovered a gene from *Mesorhizobium loti* homologous to eukaryotic $K^+$ channels of the S4 superfamily that also carry a cyclic nucleotide binding domain at the COOH terminus. The gene was cloned from genomic DNA, and the protein, denoted MloK1, was overexpressed in *Escherichia coli* and purified. Gel filtration analysis revealed a heterogeneous distribution of protein sizes which, upon inclusion of cyclic nucleotide, coalesces into a homogeneous population, eluting at the size expected for a homotetramer. As followed by a radioactive $^{86}Rb^+$ flux assay, the putative channel protein catalyzes ionic flux with a selectivity expected for a $K^+$ channel. Ion transport is stimulated by cAMP and cGMP at submicromolar concentrations. Since this bacterial homologue does not have the "C-linker" sequence found in all eukaryotic S4-type cyclic nucleotide-modulated ion channels, these results show that this four-helix structure is not a general requirement for transducing the cyclic nucleotide-binding signal to channel opening.

KEY WORDS: transport • reconstitution • flux • HCN • CNG



## INTRODUCTION

Ion channels gated by cyclic nucleotides are widely distributed throughout eukaryotes (Kaupp and Seifert, 2002; Robinson and Siegelbaum, 2003). As the molecular hardware linking changes of intracellular cyclic nucleotide levels occurring in sensory transduction to cellular electrical responses, these proteins are especially important in the coherent functioning of electrically excitable tissues. They have been most widely studied in sensory neurons, where they carry out essential tasks in the detection of photons or odorants, in cardiac myocytes, where they underlie pacemaking activity, and in cerebellar neurons, where they contribute to fine tuning in motor-coordination circuits. All such channels belong to the S4 superfamily (Yellen, 2002; Yu and Catterall, 2003), which also includes voltage-dependent $Ca^{2+}$, $Na^+$, and $K^+$ channels; these proteins are tetramers of identical or similar subunits, or of honorary subunits inhabiting the same polypeptide in tandem, with each subunit having six transmembrane sequences and a pore-forming sequence positioned between the fifth and sixth of these.

The cyclic nucleotide-modulated channels additionally carry a cyclic nucleotide-binding domain (CNBD) in the cytoplasmic COOH-terminal region. These channels fall operationally into two broad subclasses, denoted CNG (cyclic nucleotide gated) and HCN (hyperpolarization and cyclic nucleotide activated). Channels of the first class depend absolutely on cyclic nucleotides for opening, gate in a voltage-independent manner, and permit conduction only by monovalent cations, with little ionic selectivity among the group IA cations. In contrast, HCN channels are merely modulated by cyclic nucleotides in their primary mode of voltage-dependent gating, and, while also conductive to monovalent cations, favor $K^+$ over $Na^+$ by a factor of approximately four. At the molecular level, both CNG and HCN channels show the arginine-decorated fourth transmembrane sequence characteristic of the S4 family, and both carry similar CNBD sequences. In keeping with their $K^+$ selectivity, HCN channels carry the "GYG" pore-forming selectivity sequence unique and common to $K^+$ channels (Heginbotham et al., 1992), while CNG channels lack this sequence.

The recent high-resolution structures of several $K^+$ channels (Doyle et al., 1998; Jiang et al., 2002, 2003) provide an outline of molecular architecture in this protein family but leave many questions specific to the cyclic nucleotide-binding subfamily unaddressed. Are these, like $K^+$ channels, built as fourfold symmetric structures, as in the structure of an isolated CNBD of an HCN channel (Zagotta et al., 2003), or as dimers-of-dimers, as suggested by functional experiments on CNG and HCN channels (Liu et al., 1998; Ulens and Siegelbaum, 2003)? What accounts for the hyperpolarization-dependent opening of HCN channels, a voltage dependence with polarity opposite to that of conventional $K_v$-type $K^+$ channels (Mannikko et al., 2002)? How does the "C-linker," the ~80-residue sequence

Address correspondence to Crina M. Nimigean, Department of Biochemistry, Howard Hughes Medical Institute, Brandeis University, 415 South St., Waltham, MA 02454. Fax: (781) 736-2365; email: cnimigea@brandeis.edu

*Abbreviations used in this paper:* CNBD, cyclic nucleotide-binding domain; CNG, cyclic nucleotide gated; HCN, hyperpolarization and cyclic nucleotide activated; NMG, *N*-methyl glucamine.


J. Gen. Physiol. © The Rockefeller University Press • 0022-1295/2004/09/203/8 $8.00
Volume 124 September 2004 203–210
http://www.jgp.org/cgi/doi/10.1085/jgp.200409133

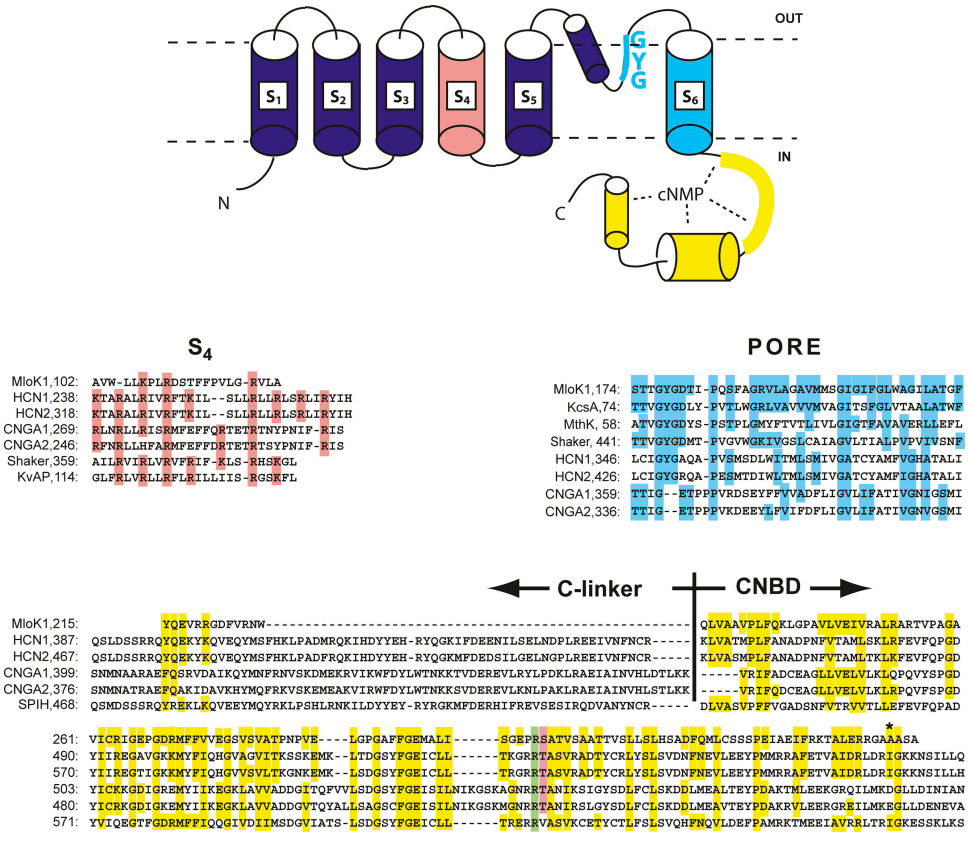


FIGURE 1. MloK1 in the S4 ion channel superfamily. Predicted transmembrane segments shown as cylinders, CNBD in yellow, pore region in cyan. Alignments are colored to correspond with transmembrane topology diagram. In CNBD, the completely conserved Arg is shown in green and the adjacent conserved hydroxy amino acid in red. Asterisk marks the position of acidic residues in CNG channels (Varnum et al., 1995) responsible for selectivity against cAMP. Channel abbreviations, with NCBI accession nos., are as follows: HCN1, mouse HCN (O88704), HCN2, human HCN (Q9UL51), CNGa1, bovine CNG (Q00194), CNGa2, bovine CNG (Q03041), SPIH, sea urchin HCN (NP999729).

connecting the CNBD to the sixth transmembrane helix, mediate between cyclic nucleotide binding and channel opening (Gordon and Zagotta, 1995)? Why, despite their $K^+$ selectivity sequence, are HCN channels so much less $K^+$ selective than other $K^+$ channels, which typically show 100–1,000-fold selectivity for $K^+$ over $Na^+$?

These questions will ultimately require structural answers. The only productive avenue toward high-resolution ion channel structure is currently provided by bacterial homologues, which in some cases allow overexpression in *Escherichia coli* of properly assembled proteins amenable to purification and crystallization. For this reason, we searched prokaryotic databases for S4-type ion channels containing cyclic nucleotide-binding domains. We now describe the overexpression, purification, and functional reconstitution of an S4-superfamily homologue from *Mesorhizobium loti*, with a $K^+$ selectivity sequence and a CNBD. The channel's chromatographic behavior in detergent micelles and its ionic flux properties in liposomes respond to micromolar levels of cyclic nucleotides, and its selectivity for $K^+$ is higher than that of either CNG or HCN subtypes.

## MATERIALS AND METHODS

### *Biochemical*

A putative bacterial channel protein homologous to eukaryotic cyclic nucleotide-gated channels was identified by a homology search of the TIGR bacterial database. The coding sequence was PCR cloned from *M. loti* genomic DNA and inserted into an *E. coli* expression vector (pASK-IBA2; Sigma-Genosys) with a COOH-terminal hexahistidine tag. *E. coli* JM83 were transformed with this construct, and after plating on LB-Amp, cells were harvested and grown in Terrific Broth. Expression of protein was induced for 90 min with 0.2 mg/L anhydrotetracycline at a cell density ($A_{550}$) of 1.0. Cells were pelleted, resuspended in 100 mM KCl, 50 mM tris-HCl, pH 7.5 (50 ml for 1–3 liter culture), and lysed by sonication on ice in the presence of protease inhibitors (complete EDTA-free, Roche, and PMSF 0.17 mg/ml). All subsequent steps were performed at room temperature. Membrane protein was extracted 2 h by adding 50 mM *n*-decylmaltoside (DM; Anatrace), and the extract, clarified by centrifugation, was applied to a $Ni^{2+}$ affinity column (QIAGEN). After washing off nonspecifically bound proteins with running buffer (100 mM KCl, 20 mM Tris-HCl, 5 mM DM, pH 7.6) supplemented with 40 mM imidazole, the protein was eluted by raising imidazole to 400 mM, concentrated to 8–15 mg/ml in Amicon ultracentrifugal concentrators, and chromatographed on a Superdex 200 size exclusion column (Amersham Biosciences) in running buffer. When needed, cyclic adenosine monophosphate or cyclic guanosine monophosphate (cAMP, cGMP, Fluka), 50–200 μM unless otherwise specified, was added to the bacterial suspension before sonication and maintained during all purification and reconstitution steps. In experiments in which cyclic nucleotide concentration was varied, protein was always prepared in high cyclic nucleotide, and the desired final concentration was introduced in the reconstitution step. Eluted protein was analyzed by SDS-PAGE gel electrophoresis and the proteins visualized by Coomassie staining.

The purified protein was immediately reconstituted into liposomes at a concentration of 0.1–50 μg protein/mg lipid in 20

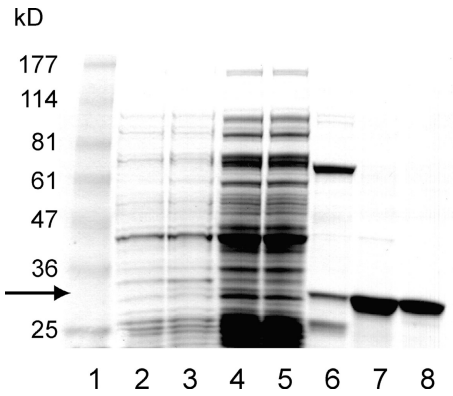


FIGURE 2. Overexpression and purification of MloK1. Protein samples were run on a 10% polyacrylamide SDS gel stained with Coomassie blue as follows: lane 1, protein ladder with molecular weights indicated; lanes 2 and 3, pre- and post-induction whole *E. coli* lysates; lane 4, clarified membrane extract of induced cells; lane 5, $Ni^{2+}$ column flow-through of membrane extract; lane 6, nonspecifically bound protein wash of $Ni^{2+}$ column; lane 7, $Ni^{2+}$ column–eluted MloK1 (7 μg); lane 8, gel filtration column-purified MloK1 (7 μg). Arrow indicates position of purified MloK1 protein.

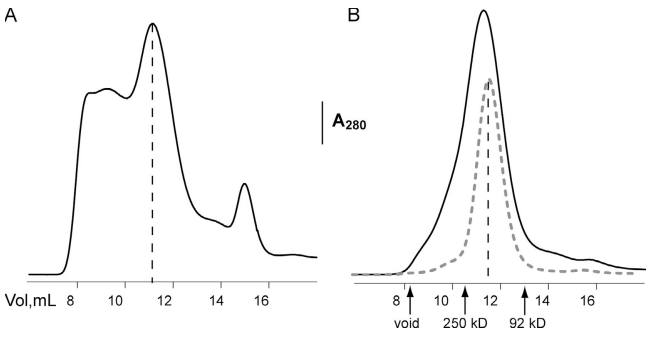


FIGURE 3. Gel filtration chromatography of MloK1. Preparations of $Ni^{2+}$ column–purified (solid curve) or gel filtration–purified (dashed curve in B) MloK1 were applied to a Superdex gel filtration column monitored at 280 nm in the absence (A) or presence (B) of 50 μM cAMP. Dashed lines mark the tetrameric MloK1 peak and arrows indicate the void volume and molecular weights of two calibrated membrane proteins run under identical conditions: MthK $K^+$ channel tetramer (250 kD) and CLC-ecl $Cl^-$ transporter dimer (92 kD). According to a calibration using five membrane proteins of known sizes run under identical conditions, the elution volume of MloK1 corresponds to ~150 kD. Scale bar for absorbance at 280 nm represents 20 mAU for A and 100 mAU for B.

mg/ml *E. coli* polar lipids (Avanti Polar Lipids, Inc.) in the presence or absence of cAMP or cGMP. Detergent was removed either by overnight dialysis against ~1,000 volumes of 400 mM KCl, 10 mM Hepes, 5 mM *N*-methyl glucamine (NMG), pH 7.6, or by chromatography on Sephadex G-50 fine, equilibrated in this same solution. The recovered liposomes were frozen in liquid $N_2$ and stored at −80°C.

### *Flux Assays*

The $^{86}Rb^+$ flux assay has been described in detail (Heginbotham et al., 1998). In brief, liposomes were thawed, sonicated, and passed over G-50 spin-columns (100 μL liposome, 1.5 ml column) equilibrated in uptake buffer (400 mM sorbitol, 50 μM KCl, 10 mM Hepes, 5 mM NMG, and the desired concentration of cAMP or cGMP) to establish a $K^+$ gradient across the liposome membrane. Uptake of $^{86}Rb^+$ was initiated by mixing the liposomes with two to six volumes of uptake buffer containing trace amounts of $^{86}Rb^+$ (~0.1 μCi/ml), as depicted in the inset of Fig. 4. At each time point, extraliposomal $^{86}Rb^+$ was removed by passing a 100 μL aliquot over a 1.5-ml cation-exchange Dowex column (50WX4-100; Sigma-Aldrich) converted to the $NMG^+$ form, and radioactivity was measured in a liquid scintillation counter. Valinomycin (1 μg/ml) was added at the end of each experiment to assay maximum $^{86}Rb^+$ uptake into all liposomes present.

To follow proton uptake into electrically polarized liposomes, protein-free or reconstituted vesicles were thawed and supplemented with 50 mM $KP_i$, pH 7.3, and were then sonicated 5–10 s to trap the buffer in the internal space. For each assay, 100 μL of vesicles was applied to a 1.5-ml spin column equilibrated with proton uptake solution (350 mM NaCl, 10 mM KCl, 2 mM $KP_i$, pH 7.3) to exchange the external solution and establish a $K^+$ gradient. The liposomes (100 μL) were immediately diluted into a stirred vial containing 1.9 ml of proton uptake solution, in which a pH electrode was positioned. The pH of the solution was recorded on chart paper on a high-sensitivity scale (~0.06 pH units full scale). FCCP and valinomycin were used to permeabilize the liposomes to $H^+$ and $K^+$, respectively.

## RESULTS

In a BLAST search for S4-type channels containing CNBDs, we noticed, among four other hits, a putative $K^+$ channel homologue in the plant symbiont *M. loti*, an organism commonly used for genetic studies of rhizobial symbiosis and nitrogen fixation. The gene (GenBank/EMBL/DDBJ accession no. NP104392) encodes a 355-residue polypeptide of 38 kD with six putative transmembrane sequences (S1–S6), where S4 bears three basic residues (two arginines, one lysine), a $K^+$ selectivity sequence (TTGYGD) between S5 and S6, and a COOH-terminal CNBD (Fig. 1). The pore sequence for this protein, which we call MloK1, is homologous to the corresponding region of other $K^+$ channels such as KcsA (60% identity) and Shaker (50%), and its CNBD displays convincing similarity (~30%) to those of eukaryotic CNG and HCN subtypes. Unlike its eukaryotic counterparts, MloK1 does not contain the four-helix C-linker domain, which connects the end of S6 to the CNBD and is thought to transmit the cyclic nucleotide binding signal to the channel's gate (Gordon and Zagotta, 1995; Zong et al., 1998; Paoletti et al., 1999; Johnson and Zagotta, 2001; Wang et al., 2001). In MloK1, the CNBD sequence begins only 13 residues after S6 emerges from the membrane.

The channel protein, engineered with a COOH-terminal His6 tag and placed behind a tetracycline promoter, is efficiently expressed in *E. coli* (Fig. 2), with an induction-dependent band of ~35 kD visible on SDS-PAGE even in the whole-cell lysate. After extraction of the cells in detergent, high purity is achieved in a single pass over a $Ni^{2+}$-chelate column with a yield of ~3 mg/L

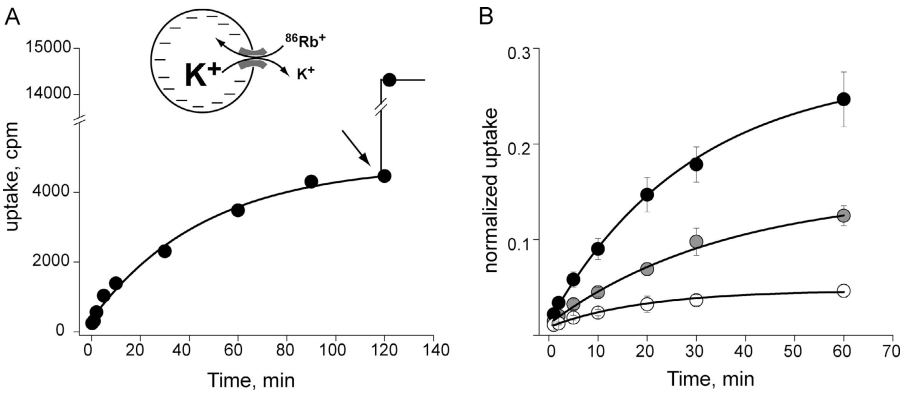


FIGURE 4. Concentrative $^{86}Rb^+$ uptake by MloK1. (A) Representative time course of accumulation of $^{86}Rb^+$ into liposomes reconstituted with MloK1 (10 μg/mg lipid, 200 μM cAMP). Each point represents radioactivity of a single 100-μl sample removed from the reaction mix at the time point indicated. After the 2-h sample was collected, valinomycin was added (arrow) and a sample was taken 2 min later. (B) Valinomycin-normalized $^{86}Rb^+$ uptake in liposomes reconstituted with MloK1 (10 μg/mg lipid) in the presence of cAMP (200 μM, black circles) or in its absence (gray circles). Unfilled circles represent background $^{86}Rb^+$ uptake in protein-free liposomes. Symbols represent mean ± SEM of at least three different experiments. Smooth curves carry no theoretical meaning. Inset, cartoon of $^{86}Rb^+$ uptake assay, with liposomes loaded with high $K^+$ (400 mM) immersed in low $K^+$ solution (50 μM) containing tracer $Rb^+$; this leads to a high negative intraliposomal potential, which the $Rb^+$ tracer follows (Heginbotham et al., 1998).

culture. The chromatographic behavior of the affinity-purified protein on gel filtration is cyclic nucleotide dependent (Fig. 3). In the absence of cyclic nucleotide, much of the protein elutes as an aggregate in the void volume, with some tetrameric material (~150 kD) following, along with several other peaks. However, with 50 μM cAMP present, most of the material runs as a single tetrameric peak, as though the protein population is monodisperse under this condition. Although gel filtration chromatography does not rigorously determine particle size, we are reasonably confident of our measurement here, since the column was calibrated with six membrane proteins of known size, run under identical detergent conditions. We note that these experiments were performed on two separate preparations processed in parallel in which the protein was extracted, purified, and chromatographed in the presence or absence of cAMP. cGMP supports this chromatographic propriety as well (unpublished data). This result implies that occupancy of the CNBD by ligand promotes native folding and perhaps stabilizes the channel during the purification procedure; we have found (unpublished data) that the tetrameric peak purified without cAMP and maintained in its absence remains tetrameric for at least 7 d at 4°C.

Does MloK1 function as a cyclic nucleotide-gated ion channel? We reconstituted the protein into liposomes and examined its ability to catalyze transmembrane movement of $^{86}Rb^+$, a convenient radioactive $K^+$ analogue. Influx was followed under conditions wherein liposomes loaded with high KCl are suspended in low KCl solution containing radioactive tracer, a circumstance that leads to concentrative accumulation of radioactivity. Under these conditions, significant tracer uptake can occur only in liposomes that are permeable to $K^+$ but not to $Cl^-$ (Heginbotham et al., 1998). Fig. 4 A illustrates a typical influx time course, in which $^{86}Rb^+$ becomes trapped within the liposomes with approximately exponential time dependence characterized by a half-time of ~30 min. However, even on the long, 2-h time scale of this experiment, the influx does not reach completion, and so the equilibrium level of trapped $^{86}Rb^+$ remains uncertain. We measure the maximum capacity of $^{86}Rb^+$ uptake by adding valinomycin, an ionophore which instantly permeabilizes all liposomes to $K^+$ and $Rb^+$. Thus, in this experiment, MloK1 catalyzes

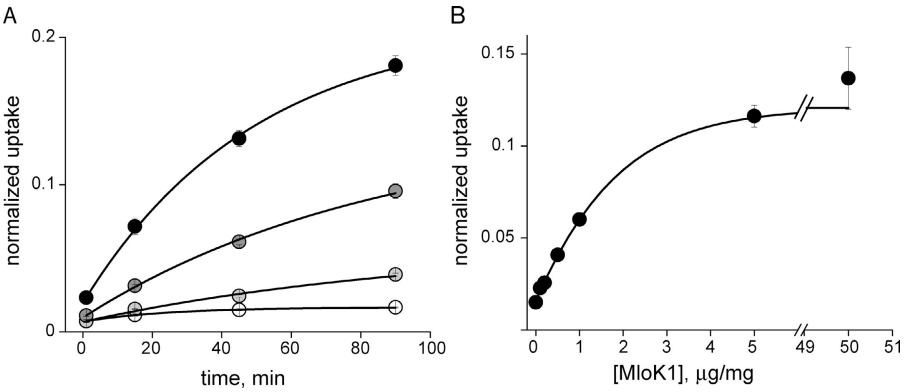


FIGURE 5. $^{86}Rb^+$ uptake is dependent on protein concentration. (A) Valinomycin-normalized $^{86}Rb^+$ uptake time course for 0 (white), 0.1 (light gray), 1 (dark gray), and 5 (black) μg MloK1/mg lipid in the presence of 50 μM cAMP. (B) Protein concentration dependence of $^{86}Rb^+$ uptake. Each time point represents $^{86}Rb^+$ accumulation after 45 min in liposomes containing MloK1 at the indicated concentrations and in the presence of 50 μM cAMP. Symbols represent mean ± SEM for three different experiments.

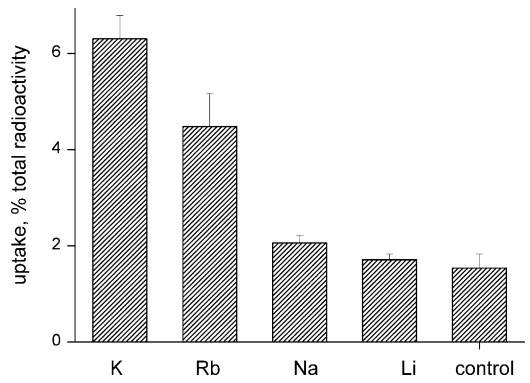


FIGURE 6. Ionic selectivity of MloK1-mediated $^{86}Rb^+$ uptake. Each bar represents $^{86}Rb^+$ uptake into liposomes reconstituted with 5 μg protein/mg lipid measured after 45 min of uptake and normalized to the total amount of radioactivity in the sample. Reconstituted liposomes were formed in the presence of the 400 mM of the $Cl^-$ salts of the indicated cations, along with of 50 μM cAMP. Bars represent mean ± SEM for 7–12 different experiments.

$^{86}Rb^+$ uptake into ~35% of the liposome space in 2 h, but because of the slowness of the time course, we cannot claim that this represents the fraction of liposomes carrying functional MloK1; it does place a lower limit on this fraction, however. Henceforth we normalize influx time courses to the maximum uptake measured by valinomycin to compare results obtained from different reconstitution conditions, as in Fig. 4 B. Here, the effect of cAMP on influx is shown. Over the ~1-h time course, a small background uptake occurs in protein-free liposomes. Reconstitution of MloK1 increases the initial rate of uptake, and a maximal concentration of cAMP (200 μM) approximately doubles this. These results show that MloK1-mediated ion transport is not absolutely dependent on cAMP, but that the ligand enhances the protein's intrinsic activity.

The rate of $^{86}Rb^+$ uptake increases with the density of channels in the reconstituted membranes (Fig. 5). At low protein density (<2 μg protein/mg lipid), uptake increases linearly, as liposomes in excess are titrated with channel protein. Eventually, uptake levels off at high protein density >5 μg/mg (Fig. 5 B), as channel protein increases in excess of the liposomes. Unfortunately, this effect cannot be quantified, as has been done by Poisson statistics in other liposome systems (Goldberg and Miller, 1991; Heginbotham et al., 1998; Maduke et al., 1999), since the final steady level of $^{86}Rb^+$ uptake cannot be accurately determined here; nonetheless, the value of the half-saturation density (~1 μg/mg) indicates that a large fraction of the protein is functionally active, since it is at this density that the number of liposomes is roughly equal to the number of protein molecules present in the reconstitution mix (Heginbotham et al., 1998).

The appearance of a $K^+$ selectivity sequence (TTGYGD) between S5 and S6 suggests strongly that MloK1 should show a familiar $K^+$ selectivity profile, permitting permeation by $K^+$ and $Rb^+$ and effectively barring $Na^+$ and $Li^+$. To test this expectation, we adapted the concentrative uptake assay to assess ion selectivity, comparing $^{86}Rb^+$ uptake into liposomes loaded with different test cations in the presence of cAMP (Fig. 6). Uptake is similar in $K^+$ and $Rb^+$, while neither $Na^+$ nor $Li^+$ supports significant uptake. These experiments do not allow precise estimates of ionic permeability ratios, but it is clear that $Rb^+$ influx rate is close to the $K^+$ rate, and $Na^+$ and $Li^+$ permeate, if at all, at much lower rates.

Cyclic nucleotides bias the open–closed equilibrium of eukaryotic CNG and HCN channels toward open conformations. This behavior is mirrored in MloK1, although the maximum stimulatory effect of cAMP is only twofold (Fig. 4). To examine the ligand dependence of this effect, we reconstituted the channel into liposomes and used the uptake assay to determine dose–response curves for cAMP and cGMP. $^{86}Rb^+$ flux time courses in the presence of varying cyclic nucleotide concentrations are shown in Fig. 7 (A and B). Both cAMP and cGMP stimulate the uptake, and both give similar approximately twofold maximal stimulation. Dose–response curves were derived from these time courses by normalizing the uptake values measured at 15 or 45 min to the corresponding isochronal uptake at maximal ligand concentration. These follow a simple Langmuir-type concentration dependence (Hill coefficient of unity), with cAMP being ~10-fold more effective than cGMP ($K_{1/2}$ = 60 and 600 nM, respectively).

The uptake experiments above demonstrate that MloK1 mediates membrane transport for $Rb^+$ and $K^+$ but do not distinguish between electrically conductive ion movement, as would be expected for a channel homologue, and an electroneutral mechanism. The preferred way of demonstrating a conductive mechanism is to reconstitute the protein into planar lipid bilayers and record electrical currents; however, we have been so far unable to do this. We can nevertheless address this question by an alternative method using liposomes. The method employs proton uptake to report on the electrical potential set up across the liposome membrane by a $K^+$ gradient. The principle is illustrated in the cartoon of Fig. 8 A; liposomes loaded with high $K^+$ are suspended in low $K^+$ solution, and the pH of the suspension is recorded. A $K^+$-selective conductance present in the membrane produces a negative-inside electrical potential that attracts protons into the intraliposomal space. The proton-impermeable liposome membrane does not allow protons to "follow" this potential, but treatment with a proton ionophore re-

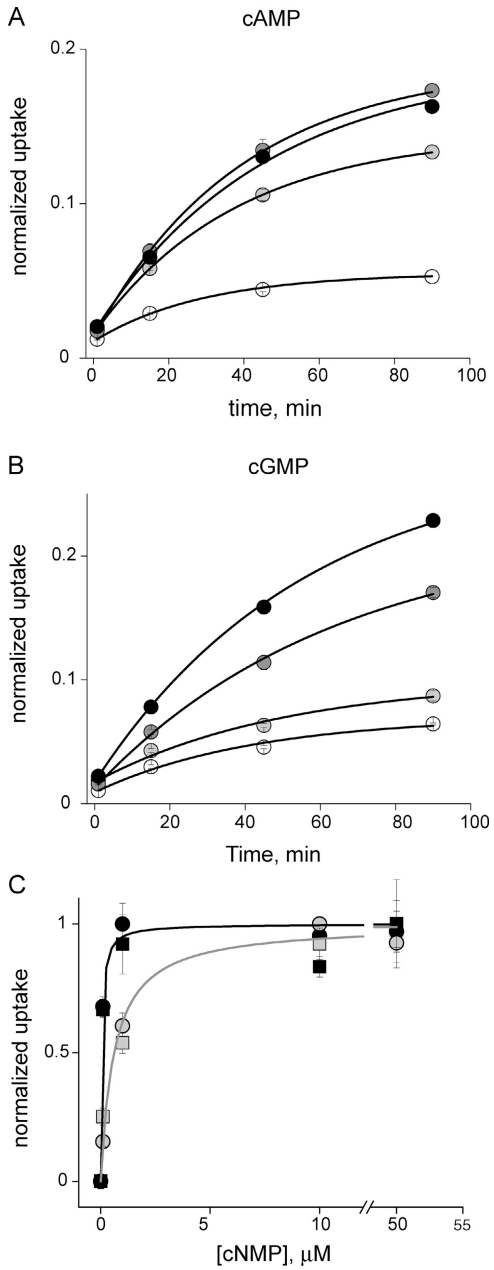


FIGURE 7. Cyclic nucleotide dependence of $^{86}Rb^+$ uptake. Flux time courses into liposomes reconstituted with 5 μg MloK1/mg lipid in the presence of cAMP (A) and cGMP (B), at 0 (white), 0.1 (light gray), 1 (dark gray), and 10 (black) μM concentration. (C) Cyclic nucleotide dose dependence of $^{86}Rb^+$ uptake. Uptake values at 15 min (squares) and 45 min (circles) are normalized to both maximum (saturating concentration of cNMP) and minimum (no cNMP) values. Smooth curves are drawn according to single-site binding functions, with $K_{1/2}$ = 60 nM for cAMP (black) and 600 nM for cGMP (gray). Each symbol represents mean ± SEM for three different experiments.

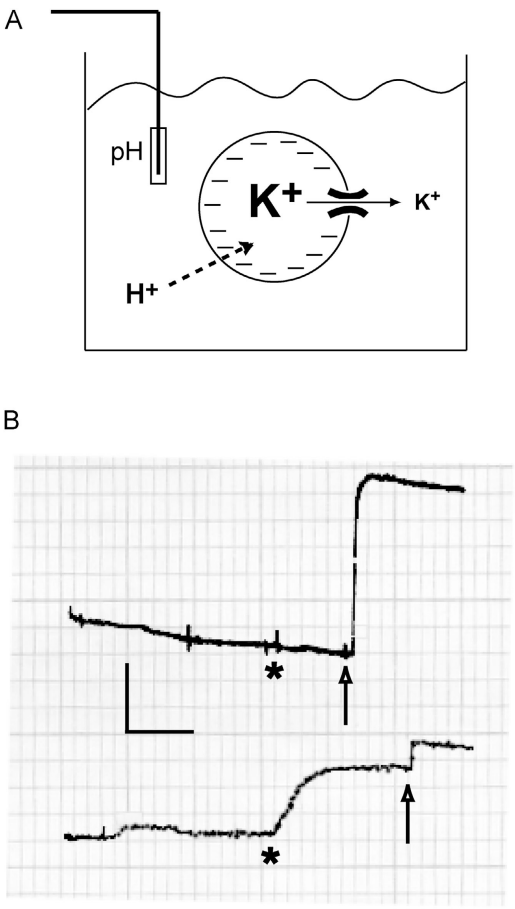


FIGURE 8. MloK1-mediated $K^+$ flux is conductive. (A) Cartoon of the method. Liposomes are loaded with high $K^+$ and suspended in low $K^+$, with a $K^+$-specific conductance present in the membrane. Under these conditions, the membrane becomes polarized, inside negative. If a proton ionophore is present to circumvent the impermeability of the lipid bilayer, protons will be drawn into the liposomes to "follow" the electrical potential set up by the $K^+$ gradient. (B) Demonstration of electrically driven proton uptake in MloK1-reconstituted liposomes. Vesicles (20 mg/ml) loaded with high $K^+$ (450 mM) were diluted 20-fold into lightly buffered low $K^+$ (10 mM) medium, and pH was recorded. At asterisk, FCCP (0.05–0.5 μg/ml), and at arrow, valinomycin (0.5 μg/ml) were added. Top, protein-free liposomes. Bottom, liposomes reconstituted with 5 μg protein/mg lipid. Horizontal scale bar, 30 s; vertical scale bar, 13 nmol $H^+$, 0.003 pH units. Upward deflection represents pH increase in external solution.

moves this kinetic constraint and allows protons to enter, as may be observed by a pH increase in the external solution. We performed this experiment first with protein-free liposomes (Fig. 8 B, top). Addition of the weak-acid uncoupler FCCP, which permeabilizes the membranes specifically to protons, has no effect on the pH of the suspension by itself. Addition of the $K^+$-specific ionophore valinomycin polarizes the membrane and produces an immediate rise in pH, as protons are taken up against a pH gradient but down their electrical gradient. When this experiment is repeated on liposomes reconstituted with MloK1, however, FCCP causes prompt $H^+$ influx without addition of valinomycin (Fig. 8 B, bottom). Thus, MloK1 substitutes functionally for valinomycin in setting up a negative internal

membrane potential, and is therefore conductive, not electroneutral. The experiment further shows that MloK1 is selective for $K^+$ over both $Na^+$ and $H^+$. Subsequent addition of valinomycin causes only a small additional pH increase, as though <25% of the liposomes in the population are free of functional MloK1 protein. These pH responses are completely abolished in the absence of a $K^+$ gradient (unpublished data).

## DISCUSSION

All structures of ion channels determined so far have been prokaryotic in origin, mainly because of the empirical and tragic fact that overexpression of eukaryotic integral membrane proteins in *E. coli* has been so reliably unsuccessful. For this reason, if we wish to know what a eukaryotic channel protein looks like, we are currently forced into the unsatisfactory but practical necessity of seeking bacterial or archeal homologues of the channel of interest. In such a search we found five putative S4-type ion channels of the cyclic nucleotide-binding subclass. In striking contrast to the abundance of other channel families among bacterial genomes, such as $K_v$ and $K_{ir}$ $K^+$ channels and CLC $Cl^-$ channels, these CNBD-containing homologues are rare, so far found only in five bacterial genomes, three of which are rhizobial symbionts. In no case is the biological function of any of these prokaryotic channels known.

We chose to focus on MloK1, which expresses well in *E. coli* and may be readily purified in quantity. To maintain the protein in a homogenous tetrameric state, it is necessary to keep cyclic nucleotide present throughout all steps of the purification procedure. The purified protein reconstituted into liposomes catalyzes $^{86}Rb^+$ uptake in a cyclic nucleotide-stimulated fashion. These two phenomena, along with the low concentration range in which the ligands act, imply that the COOH-terminal CNBD is properly folded and functionally competent. Furthermore, the tetrameric nature and $K^+$-like ionic selectivity of conductive fluxes are as expected for a $K^+$ channel. For these reasons, we consider that the purified MloK1 protein, in fulfilling the expectations of its sequence, is correctly folded and functional.

To which subtype of cyclic nucleotide binding channel does MloK1 belong: CNG or HCN? It is certainly not of the CNG subtype, since it is $K^+$ selective and shows a $K^+$ signature sequence. We are tempted to assign it to the HCN subfamily, on the basis of this $K^+$ selectivity, as well as the substantial basal activity in the absence of cyclic nucleotides. But in fact we cannot definitively assert that the channel is of HCN subtype. Since we have not been able to record electrical currents from MloK1, we cannot gauge its voltage dependence, a fundamental defining characteristic of HCN channels. Moreover, the high selectivity of MloK1-mediated flux for $K^+$ over $Na^+$ would not be expected for a conventional HCN channel, as these are only weakly selective for $K^+$. We are therefore unwilling to assign this channel firmly to either of the categories defined in eukaryotic channels.

Both cAMP and cGMP bind to this channel, as indicated by chromatographic behavior and ion fluxes. In the flux assay, cAMP shows ~10-fold higher potency than cGMP, with the two ligands giving similar maximal effects. Several ligand-selectivity determinants have been identified in CNBDs from eukaryotic channels, from both electrophysiological analysis of CNG channels (Altenhofen et al., 1991; Varnum et al., 1995) and direct structure determination of an isolated CNBD from an HCN channel (Zagotta et al., 2003). All eukaryotic CNBDs, regardless of ligand preference, have a conserved arginine residue that coordinates the cyclic nucleotide phosphate (Zagotta et al., 2003), and this residue is also present in MloK1 (R307; Fig. 1). A threonine is always found adjacent to this arginine in eukaryotic channels that bind both cAMP and cGMP; in the structure of HCN2 CNBD, the hydroxyl group of this threonine hydrogen bonds to the N2 atom of the guanine ring, while cAMP-specific channel isoforms, such as the sea urchin HCN channel (Gauss et al., 1998), lack this hydroxyl group. In MloK1, this position uses a serine (S308), the hydroxyl of which may play an equivalent H-bonding role, permitting cGMP to bind. Finally, CNG channels that are highly selective for cGMP have an acidic residue closer to the COOH terminus (Fig. 1, asterisk), and neutralizing this residue removes the ligand selectivity (Varnum et al., 1995); MloK1 has an alanine residue here, in harmony with responsiveness to both cAMP and cGMP. On several grounds, therefore, the ligand dependence of MloK1 is consistent with expectations based on molecular determinants in its CNBD.

One feature of MloK1, however, is unexpected from precedent: the absence of a C-linker sequence, a motif found in all eukaryotic CNG and HCN channels. The C-linker domain has been proposed to transmit the ligand-binding signal to the channel's gate in S6. This proposal arose from mutagenesis studies in CNG and HCN channels (Gordon and Zagotta, 1995; Zong et al., 1998; Paoletti et al., 1999; Johnson and Zagotta, 2001; Wang et al., 2001) and was strengthened by high-resolution structures of an isolated CNBD from an HCN isoform (Zagotta et al., 2003), where most of the intersubunit contacts in the tetramer are formed by the C-linker, which is composed of four α-helices. This structure suggested that cyclic nucleotide binding drives a rearrangement of the C-linker domains, which opens the channel's ion permeation pathway. Our results refute this proposal, at least as a necessary, general mechanism of channel modulation by cyclic nucleotides, and

they suggest that a minimal linking sequence is able to substitute for this function in the prokaryotic homologue.

Finally, we should ask whether the results here prove that MloK1 is a $K^+$ channel. In fact they do not. To be sure, the gross functional characteristics of the reconstituted protein are consistent with a channel mechanism: electrically conductive transport with $K^+$-like ionic selectivity. But without a direct measurement of unitary transport rate, it is impossible to rigorously distinguish channel from transporter mechanisms, and the liposome system on which we rely does not permit an estimate of this. We note that MloK1-mediated $^{86}Rb^+$ uptake is 10–100-fold slower than the rate expected for an always-open channel with a "typical" unitary conductance in the range 10–100 pS, or than that observed under similar conditions for KcsA (Heginbotham et al., 1998). This low uptake rate might reflect a small unitary conductance or a low open probability, even when maximally activated by cyclic nucleotide, or a combination of both. In the absence of direct single-channel recording, this point must remain unresolved, but it is worth noting that eukaryotic HCN channels have extremely low single-channel currents (DiFrancesco and Mangoni, 1994). In light of its tetrameric architecture, $K^+$-selective cyclic nucleotide-modulated ion fluxes, and unambiguous membership in the S4 superfamily of ion channels, all accessible evidence implicates MloK1 as a cyclic nucleotide-modulated $K^+$ channel.

We are grateful to the Kazusa DNA Research Institute, Japan, for providing genomic DNA from *M. loti*, to Drs. A. Accardi and R. Iyer for suggestions throughout the course of this work, and W. Nguitragool for criticisms on the manuscript.

This research was supported by National Institutes of Health grant GM-31768.

Lawrence G. Palmer served as editor.

*Submitted: 21 June 2004*
*Accepted: 26 July 2004*

REFERENCES

Altenhofen, W., J. Ludwig, E. Eismann, W. Kraus, W. Bonigk, and U.B. Kaupp. 1991. Control of ligand specificity in cyclic nucleotide-gated channels from rod photoreceptors and olfactory epithelium. *Proc. Natl. Acad. Sci. USA.* 88:9868–9872.

DiFrancesco, D., and M. Mangoni. 1994. Modulation of single hyperpolarization-activated channels by cAMP in the rabbit sinoatrial node. *J. Physiol.* 474:473–482.

Doyle, D.A., J.M. Cabral, A. Pfuetzner, J.M. Kuo, J.M. Gulbis, S.L. Cohen, B.T. Chait, and R. MacKinnon. 1998. The structure of the potassium channel: molecular basis of $K^+$ conduction and selectivity. *Science.* 280:69–77.

Gauss, R., R. Seifert, and U.B. Kaupp. 1998. Molecular identification of a hyperpolarization-activated channel in sea urchin sperm. *Nature.* 393:583–587.

Goldberg, A.F.X., and C. Miller. 1991. Solubilization and functional reconstitution of a chloride channel from *Torpedo californica* electroplax. *J. Membr. Biol.* 124:199–206.

Gordon, S.E., and W.N. Zagotta. 1995. Localization of regions affecting an allosteric transition in cyclic nucleotide-activated channels. *Neuron.* 14:857–864.

Heginbotham, L., T. Abramson, and R. MacKinnon. 1992. A functional connection between the pores of distantly related ion channels as revealed by mutant $K^+$ channels. *Science.* 258:1152–1155.

Heginbotham, L., L. Kolmakova-Partensky, and C. Miller. 1998. Functional reconstitution of a prokaryotic $K^+$ channel. *J. Gen. Physiol.* 111:741–749.

Jiang, Y., A. Lee, J. Chen, M. Cadene, B.T. Chait, and R. MacKinnon. 2002. Crystal structure and mechanism of a calcium-gated potassium channel. *Nature.* 417:515–522.

Jiang, Y., A. Lee, J. Chen, V. Ruta, M. Cadene, B.T. Chait, and R. MacKinnon. 2003. X-ray structure of a voltage-dependent $K^+$ channel. *Nature.* 423:33–41.

Johnson, J.P., Jr., and W.N. Zagotta. 2001. Rotational movement during cyclic nucleotide-gated channel opening. *Nature.* 412: 917–921.

Kaupp, U.B., and R. Seifert. 2002. Cyclic nucleotide-gated ion channels. *Physiol. Rev.* 82:769–824.

Liu, D.T., G.R. Tibbs, P. Paoletti, and S.A. Siegelbaum. 1998. Constraining ligand-binding site stoichiometry suggests that a cyclic nucleotide-gated channel is composed of two functional dimers. *Neuron.* 21:235–248.

Maduke, M., D.J. Pheasant, and C. Miller. 1999. High-level expression, functional reconstitution, and quaternary structure of a prokaryotic ClC-type chloride channel. *J. Gen. Physiol.* 114:713–722.

Mannikko, R., F. Elinder, and H.P. Larsson. 2002. Voltage-sensing mechanism is conserved among ion channels gated by opposite voltages. *Nature.* 419:837–841.

Paoletti, P., E.C. Young, and S.A. Siegelbaum. 1999. C-Linker of cyclic nucleotide-gated channels controls coupling of ligand binding to channel gating. *J. Gen. Physiol.* 113:17–34.

Robinson, R.B., and S.A. Siegelbaum. 2003. Hyperpolarization-activated cation currents: from molecules to physiological function. *Annu. Rev. Physiol.* 65:453–480.

Ulens, C., and S.A. Siegelbaum. 2003. Regulation of hyperpolarization-activated HCN channels by cAMP through a gating switch in binding domain symmetry. *Neuron.* 40:959–970.

Varnum, M.D., K.D. Black, and W.N. Zagotta. 1995. Molecular mechanism for ligand discrimination of cyclic nucleotide-gated channels. *Neuron.* 15:619–625.

Wang, J., S. Chen, and S.A. Siegelbaum. 2001. Regulation of hyperpolarization-activated HCN channel gating and cAMP modulation due to interactions of COOH terminus and core transmembrane regions. *J. Gen. Physiol.* 118:237–250.

Yellen, G. 2002. The voltage-gated potassium channels and their relatives. *Nature.* 419:35–42.

Yu, F.H., and W.A. Catterall. 2003. Overview of the voltage-gated sodium channel family. *Genome Biol.* 4:207.

Zagotta, W.N., N.B. Olivier, K.D. Black, E.C. Young, R. Olson, and E. Gouaux. 2003. Structural basis for modulation and agonist specificity of HCN pacemaker channels. *Nature.* 425:200–205.

Zong, X., H. Zucker, F. Hofmann, and M. Biel. 1998. Three amino acids in the C-linker are major determinants of gating in cyclic nucleotide-gated channels. *EMBO J.* 17:353–362.